J Membrane Biol (2013) 246:199–207
DOI 10.1007/s00232-012-9521-8

Two-Dimensional Crystalline Array Formation of Glucuronide Transporter from *Escherichia coli* by the Use of Polystyrene Beads for Detergent Removal

Noriyuki Ishii

Received: 17 July 2012 / Accepted: 4 November 2012 / Published online: 28 November 2012

Abstract *n*-Dodecyl-β-D-maltoside solubilized glucuronide transporter (GusB), the product of *gusB* gene from *Escherichia coli*, was treated with Bio-Beads as an agent for removing the detergent from a micellar solution under suitable combination with dimyristoylphosphatidylcholine. Optimizing conditions led to a two-dimensional crystalline array formation of GusB. The crystalline arrays appear to have a hexagonal lattice with layer group *P*6, the unit cell dimensions of $a = b = 13.8$ nm and $\gamma = 120°$. Each stain-protruding periodic unit showed approximately 11.8 ± 0.3 nm in a diameter in the inverse Fourier-filtered image to have formed with pentameric GusB (5×49.7 kDa).

Keywords Electron microscopy · Glucuronide transporter · GusB · Membrane protein · Two-dimensional crystallization

High-resolution structural information is essential for understanding the functional mechanism of membrane transporter proteins that play physiological roles in the cell. From the analyses of their hydropathic profiles there are, so far, over 100 examples of transporters that are believed to exist as 12 α-helices folded through the membrane (Henderson 1993; Saier et al. 1999). They carry out diverse transport functions such as nutrient uptake, toxin secretion, and ion transport by several mechanisms: uniport, substrate–ion symport, substrate–ion antiport, substrate–substrate antiport, or ATP-dependent translocation (Henderson 1993).

Glucuronide transporter is a membrane protein that is known to transport glucuronides across the membrane and plays an important role in the detoxification process of metabolites. The transporter is widely distributed in prokaryotic and eukaryotic organisms (Zamek-Gliszczynski et al. 2006). The amino acid sequence of glucuronide transporter (GusB) from *Escherichia coli* has been reported (Liang et al. 2005). This hydrophobic protein consists of 457 amino acid residues, of predicted Mr 49,982. The hydropathic profile of this deduced amino acid sequence indicates that the protein is composed of 12 membrane spanning domains (α-helices) connected by hydrophilic segments with both N- and C-termini facing the cytosol (Fig. 1) (Hirokawa et al. 1998; Ishii 2010). The protein shows 26.5 % identity with the sequence of the melibiose transporter (MelB) of *E. coli* (Yazyu et al. 1984; Pourcher et al. 1995; Yousef and Guan 2009), and 23.5 % identity with the N-terminal hydrophobic portion (from 1 to 491 amino acid) of the lactose transporter (LacS) of *Streptococcus thermophilus* (Poolman et al. 1992). Besides the primary and secondary structure, very little structural information is available for the membrane transport protein (Liang et al. 2005; Ishii 2010, 2011). Thus, detailed biochemical properties and the functional mechanism of the transporter on a molecular structural level are still obscure.

For the last decade, the electron crystallography of two-dimensional (2D) protein crystals has established itself as an excellent alternative to X-ray diffraction analyses of three-dimensional (3D) crystals for the high-resolution structural analysis of membrane proteins (Fujiyoshi 2011;

N. Ishii (✉)
Biomedical Research Institute, National Institute of Advanced Industrial Science and Technology (AIST), Tsukuba Central-6 1-1-1 Higashi, Tsukuba, Ibaraki 305-8566, Japan
e-mail: ishii@ni.aist.go.jp

N. Ishii
Life Science Division, Lawrence Berkeley National Laboratory, Department of Molecular and Cell Biology, University of California, Berkeley, CA 94720, USA

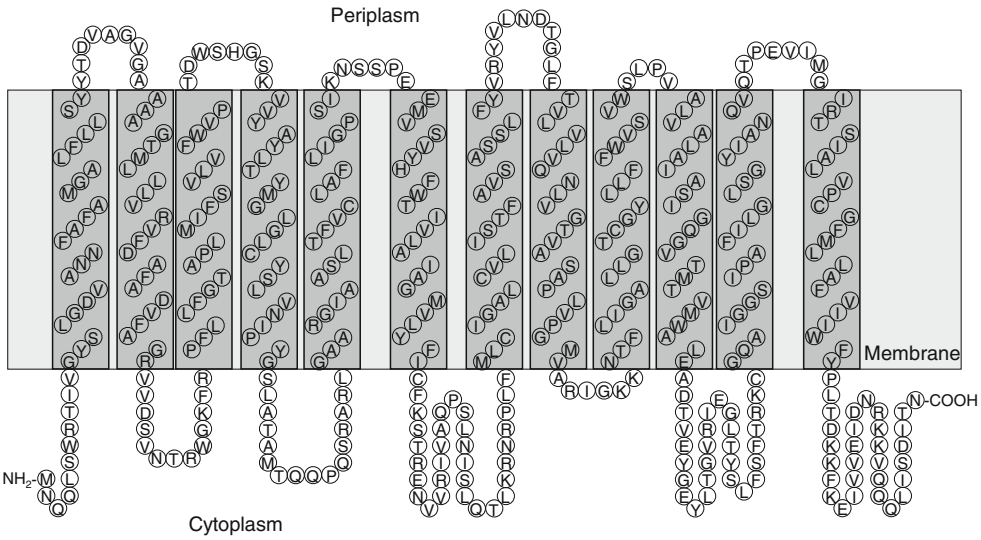

Fig. 1 Schematic drawing of the predicted secondary structure of GusB. There are 12 α-helices spanning across the membrane, with both N- and C-termini facing the cytosol

Vinothkumar and Henderson 2010). As we reported previously (Ishii 2010, 2011), size-exclusion chromatography on HPLC has proven to be an efficient method in examining and screening suitable conditions for detergent species, incubation temperature, pH, and coresiding salts. Such information are useful for maintaining the stability and mono-dispersity of the protein to achieve crystalline array formation in 2D, 3D, or helical symmetry crystallization for structural studies. Two-dimensional crystallization requires a target protein to be stable and monodisperse at the desired temperature over several days of incubation. As a result of the surface duality of being both hydrophilic and hydrophobic, membrane proteins tend to aggregate and precipitate quickly in the presence of unfavorable detergents and zwitterionic phospholipids, precluding crystalline array formation. How to maintain the stability of membrane protein to crystallization is a challenge especially for transporter proteins because they have multiple transmembrane spans and larger hydrophobic surface area. In this paper we set out to study the quaternary assembly of GusB, a system for 2D crystallization that is paradigmatic for the protein that catalyzes the transport of glucuronides, namely, conjugation with glucuronic acid possibly by ATP dependent transport processes (Liang et al. 2005). The present study has been aimed at investigating the possibility of 2D crystallization approach using Bio-Beads reported by Rigaud et al. (1997, 2000) onto GusB protein. Preliminary efforts in 2D crystalline array formation with special attention to optimizing the appropriate amounts of Bio-Beads supplied to the DDM solution containing GusB will be taken up as a core problem. Although this article is not concerned with structure analysis at high resolution, the 2D crystalline arrays obtained by the method will be shown later to be improved in combination with electron microscopic techniques to produce larger ordered flat crystals, optimizing conditions for GusB transporter such as lipids composition, presolubilization condition, incubation time, freezing and thawing crystals, and annealing crystals.

Materials and Methods

Purification of GusB

GusB with 8 histidine residues at its N-terminus was purified according to the previous report with some improvements from *E. coli* that contained multiple copies of the plasmid carrying the *gusB* gene (Ishii 2010, 2011). Briefly, the cells were collected by centrifugation, and disrupted by a French press or a ultrasonic disruptor (UD-201; Tomy Digital Biology Co., Ltd., Nerima, Tokyo). The inner membranes that contained GusB were separated from outer membranes and other components by sucrose gradient ultracentrifugation. The protein was extracted by the desired buffer containing a detergent such as 0.1 % *n*-dodecyl-β-D-maltoside (DDM) (Dojindo Molecular Technologies, Inc., Kumamoto, Japan). The protein solution was applied to a Ni-column, followed by elution with the buffer containing 10 mM HEPES–NaOH, pH 7.9, 100 mM NaCl, 20 % glucose, 0.1 % DDM, and 150 mM imidazole. The purity was examined by SDS-PAGE, and its concentration was determined by BCA protein assay method (Pierce; though Takara Bio Inc., Shiga, Japan) with bovine albumin as a standard.

Two-dimensional Crystallization of GusB and Electron Microscopy

Bio-Beads SM2 (Bio-Rad Laboratories, Inc., Hercules, CA, USA) were thoroughly rinsed first with methanol and then with Milli-Q water (Direct Q; Millipore, Billerica, MA,

USA). Meanwhile, the dry and broken beads were discarded. The beads were kept in Milli-Q water until use.

The desired amount of phospholipid either alone or as a mixture of different kinds such as phosphatidylcholine (PC), phosphatidylethanolamine (PE), dimyristoylphosphatidylcholine (DMPC), phosphatidylglycerol (PG), phosphoserine (PS), oleoylstearoylphosphatidylcholine (OSPC), dioleoylphosphatidylcholine (DOPC), dilinoleoylphosphatidylcholine (DLPC), oleoylpalmitoylphosphatidylcholine (OPPC), or *E. coli* total lipids extracts, in chloroform was put into a glass tube and dried down by nitrogen gas so that the lipids made thin layered film at the bottom of the tube. The tube was further evaporated to remove the solvent chloroform completely using the vacuum evaporator (JEOL JEE420; JEOL Ltd., Akishima, Tokyo, Japan). Then, aliquots of the detergent-solubilized purified GusB in the desired buffer composition containing 0.1 % (w/v) detergent were added and the dry lipid layer was scratched and dissolved completely on ice (Fig. 2, step I). After the incubation at 4 °C, small amounts of Bio-Beads from Milli-Q water were blotted with tissue paper to remove excess moisture. The desired amount of moist beads were weighed swiftly and added directly to the detergent-containing solutions (Fig. 2, steps II, III, and IV). The detergent was removed in the following manner either by adding small amounts of Bio-Beads at one time or by adding the same amount of the beads divided by several steps, keeping the sample solution in the incubator at the desired temperature, being gently stirred by a small magnetic bar (Fig. 2, steps II, III, IV, and V).

The condition that brought favorable results (2D crystalline array formation) is as follows; starting from a solubilized lipid-protein solution (lipid/protein = 1.1 w/w) containing 1.0 mg/ml DDM, 2D crystallization experiments were performed at 28.9 °C, by adding 1.5 mg of Bio-Beads each at three different steps with 30 min intervals to 120 μl of 0.1 % DDM solution contained 99 μg of the purified protein supplemented with 110 μg of DMPC in HEPES-Na buffer, pH 7.9. Aliquots collected at various time intervals during the course of the incubation were investigated by electron microscopy. In electron microscopy, aliquots of the sample solution were applied to glow-discharged carbon grids for 1 min, and then those were stained for 1 min with 2 % (w/v) uranylacetate. The specimen grids were examined in a FEI Tecnai 20F electron microscope (FEI Company, Eindhoven, The Netherlands) operated at 120 kV. Images were recorded at 0° tilt on Kodak SO-163 films (Eastman Kodak Company, Rochester, NY, USA) at 44,300× nominal magnification. The micrographs were digitized in a Zeiss SCAI scanner (Carl Zeiss MicroImaging GmbH, Göttingen, Germany) with a sampling window corresponding to 1.5 Å/pixel and FFT analysis was performed using DigitalMicrograph (Gatan, Inc., Pleasanton, CA, USA).

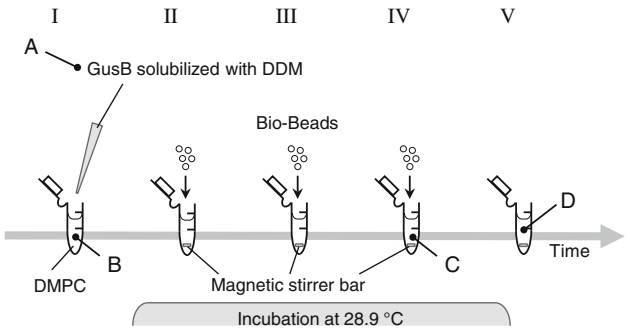

Fig. 2 Schematic drawing of the experimental procedures where the step for addition of Bio-Beads is divided into 3 with certain intervals. *Labels A–D* correspond to the electron micrographs in Fig. 3

Results

As we have shown previously (Ishii 2010, 2011), the stability dependencies of GusB against buffer species and pH, lipids, and incubation temperature were checked by the gel permeation HPLC (Shodex protein kw-804; Showa Denko, Kanagawa, Japan) for each preparation of the protein. The elution profiles were investigated carefully. Mixing ratio of the components, etc. of sample solutions for the 2D crystallization were made with reference to the results obtained from the gel permeation HPLC experiments.

Table 1 shows the typical examples of amphiphiles examined in the study effecting 2D crystalline array formation of GusB. The results of lipids other than DMPC have been described with reference to Table 1. The 2D crystallization procedure used is schematically shown in Fig. 2. Explanations for the detailed procedures at each step are described in Materials and Methods. The alphabetical labels (A–D) shown in Fig. 2 correspond to those of electron micrographs in Fig. 3. Figure 3 shows the electron micrographs that were captured as a typical image at each stage during the incubation with Bio-Beads. After the purification of the desired protein, the sample solution should consist of monodispersed protein-detergent complexes (Fig. 3a). Figure 3a shows the freshly prepared GusB protein in 0.1 % DDM, and the stacked layered structures are seen, which are typical to membrane proteins (Sato et al. 1994). The initial stage of solubilization of the membrane protein resulted in a rather heterogeneous population of aggregates containing proteins, lipids, and the detergent (Fig. 3b). In Fig. 3b, at the stage before the addition of Bio-Beads, all components of the membrane protein GusB, detergent (DDM), and lipid (DMPC) are seen gathered two-dimensionally. It appears that there is fluidity between the stacked layered structures consisting

Table 1 Typical examples of amphiphiles effecting 2D crystalline array formation of GusB

Amphiphile	Lipid/protein ratio (w/w)	Buffer condition	Effect on 2D crystalline array formation
Soybean PC	1.1	HEPES pH 7.9/4 °C, 20 °C	−
Egg PC	1.1	HEPES pH 7.9/20 °C	−
90 % PC + 10 % PG	1.1	HEPES pH 7.9/20 °C	−
90 % PE + 10 % PS	1.1	HEPES pH 7.9/20 °C	−
E. coli PE	1.1	HEPES pH 7.9/20 °C	−
90 % PE + 10 % PG	1.1	HEPES pH 7.9/20 °C	−
90 % PE + 10 % PS	1.1	HEPES pH 7.9/20 °C	−
DMPC	0.3	Acetate pH 4.8/28.9 °C	−
DMPC	0.6	Acetate pH 4.8/28.9 °C	−
DMPC	0.9	Acetate pH 4.8/28.9 °C	−
DMPC	1.1	Acetate pH 4.8/28.9 °C	−
DMPC	1.3	Acetate pH 4.8/28.9 °C	−
DMPC	0.3	Acetate pH 5.1/28.9 °C	−
DMPC	0.6	Acetate pH 5.1/28.9 °C	−
DMPC	0.9	Acetate pH 5.1/28.9 °C	−
DMPC	1.1	Acetate pH 5.1/28.9 °C	−
DMPC	1.3	Acetate pH 5.1/28.9 °C	−
DMPC	0.9	Citrate pH 4.9/28.9 °C	−
DMPC	1.1	Citrate pH 4.9/28.9 °C	−
DMPC	1.2	Citrate pH 4.9/28.9 °C	+ (stripes)
DMPC	1.3	Citrate pH 4.9/28.9 °C	+ (stripes)
DMPC	0.9	Citrate pH 5.1/28.9 °C	−
DMPC	1.1	Citrate pH 5.1/28.9 °C	−
DMPC	1.1	Citrate pH 5.6/28.9 °C	−
DMPC	1.2	Citrate pH 5.6/28.9 °C	+ (stripes)
DMPC	1.3	Citrate pH 5.6/28.9 °C	+ (stripes)
DMPC	0.9	Citrate pH 5.8/28.9 °C	−
DMPC	1.1	Citrate pH 5.8/28.9 °C	−
DMPC	1.3	Citrate pH 5.8/28.9 °C	−
DMPC	1.1	Citrate pH 6.0/28.9 °C	−
DMPC	1.2	Citrate pH 6.0/28.9 °C	−
DMPC	1.3	Citrate pH 6.0/28.9 °C	+ (stripes)
DMPC	0.9	Citrate pH 6.2/28.9 °C	−
DMPC	1.1	Citrate pH 6.2/28.9 °C	−
DMPC	1.3	Citrate pH 6.2/28.9 °C	−
DMPC	1.1	Citrate pH 6.4/28.9 °C	−
DMPC	1.2	Citrate pH 6.4/28.9 °C	+ (stripes)
DMPC	1.3	Citrate pH 6.4/28.9 °C	+ (stripes)
DMPC	0.9	Citrate phosphate pH 6.7/28.9 °C	−
DMPC	1.1	Citrate phosphate pH 6.7/28.9 °C	−
DMPC	1.3	Citrate phosphate pH 6.7/28.9 °C	−
DMPC	0.9	Citrate phosphate pH 7.2/28.9 °C	−
DMPC	1.1	Citrate phosphate pH 7.2/28.9 °C	−
DMPC	1.3	Citrate phosphate pH 7.2/28.9 °C	−
DMPC	0.6	MES pH 6.2/28.9 °C	−
DMPC	0.9	MES pH 6.2/28.9 °C	−
DMPC	1.1	MES pH 6.2/28.9 °C	−
DMPC	1.3	MES pH 6.2/28.9 °C	−

Table 1 continued

Amphiphile	Lipid/protein ratio (w/w)	Buffer condition	Effect on 2D crystalline array formation
DMPC	0.6	MES pH 6.5/28.9 °C	−
DMPC	0.9	MES pH 6.5/28.9 °C	−
DMPC	1.1	MES pH 6.5/28.9 °C	−
DMPC	1.3	MES pH 6.5/28.9 °C	−
DMPC	0.6	MES pH 6.9/28.9 °C	−
DMPC	0.9	MES pH 6.9/28.9 °C	−
DMPC	1.1	MES pH 6.9/28.9 °C	−
DMPC	1.3	MES pH 6.9/28.9 °C	−
DMPC	0.9	HEPES pH 7.0/28.9 °C	−
DMPC	1.1	HEPES pH 7.0/28.9 °C	−
DMPC	1.3	HEPES pH 7.0/28.9 °C	−
DMPC	0.9	HEPES pH 7.2/28.9 °C	+ (stripes)
DMPC	1.1	HEPES pH 7.2/28.9 °C	+ (stripes)
DMPC	1.3	HEPES pH 7.2/28.9 °C	−
DMPC	0.9	HEPES pH 7.4/28.9 °C	−
DMPC	1.1	HEPES pH 7.4/28.9 °C	+ (stripes)
DMPC	1.3	HEPES pH 7.4/28.9 °C	+ (stripes)
DMPC	0.9	HEPES pH 7.6/28.9 °C	−
DMPC	1.1	HEPES pH 7.6/28.9 °C	+ (stripes)
DMPC	1.3	HEPES pH 7.6/28.9 °C	+ (stripes)
DMPC	0.9	HEPES pH 7.8/28.9 °C	−
DMPC	1.1	HEPES pH 7.8/28.9 °C	−
DMPC	1.3	HEPES pH 7.8/28.9 °C	−
DMPC	0.7	HEPES pH 7.9/28.9 °C	−
DMPC	1.1	HEPES pH 7.9/28.9 °C	+++ (2D crystalline arrays)
DMPC	1.2	HEPES pH 7.9/28.9 °C	++ (2D crystalline arrays)
90 % DMPC + 10 % PC	1.1	HEPES pH 7.9/28.9 °C	−
80 % DMPC + 20 % PC	1.1	HEPES pH 7.9/28.9 °C	−
90 % DMPC + 10 % PG	1.1	HEPES pH 7.9/28.9 °C	−
80 % DMPC + 20 % PG	1.1	HEPES pH 7.9/28.9 °C	−
90 % DMPC + 10 % PS	1.1	HEPES pH 7.9/28.9 °C	−
80 % DMPC + 20 % PS	1.1	HEPES pH 7.9/28.9 °C	−
90 % DMPC + 10 % PE	1.1	HEPES pH 7.9/28.9 °C	+ (stripes)
80 % DMPC + 20 % PE	1.1	HEPES pH 7.9/28.9 °C	−
90 % DMPC + 10 % OSPC	1.1	HEPES pH 7.9/28.9 °C	−
80 % DMPC + 20 % OSPC	1.1	HEPES pH 7.9/28.9 °C	−
90 % DMPC + 10 % DOPC	1.1	HEPES pH 7.9/28.9 °C	−
80 % DMPC + 20 % DOPC	1.1	HEPES pH 7.9/28.9 °C	−
90 % DMPC + 10 % DLPC	1.1	HEPES pH 7.9/28.9 °C	−
80 % DMPC + 20 % DLPC	1.1	HEPES pH 7.9/28.9 °C	−
90 % DMPC + 10 % OPPC	1.1	HEPES pH 7.9/28.9 °C	−
80 % DMPC + 20 % OPPC	1.1	HEPES pH 7.9/28.9 °C	−
DOPC	0.9	Citrate phosphate pH 6.7/4 °C, 20 °C	−
DOPC	1.1	Citrate phosphate pH 6.7/4 °C, 20 °C	−
DOPC	1.3	Citrate phosphate pH 6.7/4 °C, 20 °C	−
DOPC	1.1	Citrate phosphate pH 7.2/4 °C, 20 °C	−
DOPC	0.8	HEPES pH 7.9/4 °C, 20 °C	−
DOPC	1.0	HEPES pH 7.9/4 °C, 20 °C	−

Table 1 continued

Amphiphile	Lipid/protein ratio (w/w)	Buffer condition	Effect on 2D crystalline array formation
DOPC	1.1	HEPES pH 7.9/4 °C, 20 °C	–
DOPC	1.2	HEPES pH 7.9/4 °C, 20 °C	–
DLPC	1.1	HEPES pH 7.9/4 °C, 20 °C	–
E. coli total lipids	0.5	Citrate pH 5.0/24 °C	–
E. coli total lipids	0.8	Citrate pH 5.0/24 °C	–
E. coli total lipids	1.1	Citrate pH 5.0/24 °C	–
E. coli total lipids	0.1	Citrate pH 5.5/25 °C	–
E. coli total lipids	0.3	Citrate pH 5.5/25 °C	–
E. coli total lipids	0.5	Citrate pH 5.5/24 °C, 25 °C	–
E. coli total lipids	0.8	Citrate pH 5.5/24 °C	–
E. coli total lipids	1.1	Citrate pH 5.5/24 °C	–
E. coli total lipids	0.1	Citrate pH 6.0/25 °C	–
E. coli total lipids	0.3	Citrate pH 6.0/25 °C	–
E. coli total lipids	0.5	Citrate pH 6.0/24 °C, 25 °C	–
E. coli total lipids	0.8	Citrate pH 6.0/24 °C	+ (stripes)
E. coli total lipids	1.1	Citrate pH 6.0/24 °C	–
E. coli total lipids	1.1	HEPES pH 7.9/24 °C, 25 °C	–
E. coli total lipids	1.5	HEPES pH 7.9/24 °C, 25 °C	–

Bio-Beads divided into 3 were added to each solution of about 1.5 mg, respectively

PC phosphatidylcholine, *PE* phosphatidylethanolamine, *DMPC* dimyristoylphosphatidylcholine, *PG* phosphatidylglycerol, *PS* phosphoserine, *OSPC* oleoylstearoylphosphatidylcholine, *DOPC* dioleoylphosphatidylcholine, *DLPC* dilinoleoylphosphatidylcholine, *OPPC* oleoylpalmitoyl phosphatidylcholine

of the membrane protein. After two times of 30 min-incubation with Bio-Beads, vesicles of approximately 500 nm in diameter were observed (Fig. 3c). They appeared to grow gradually into larger aggregated vesicles with densely packed particles in the following 30 min or 1 h incubation at 28.9 °C (data not shown). Prolonged incubation led to numerous large round vesicles in 0.5–1 μm in diameter, which contained some regions of crystallinity of the transporter (Figs. 3c, 4). Some crystalline arrays occasionally showed structural order with computed FFT beyond 3.4 nm resolution (data not shown). However, further prolonged incubation in the presence of Bio-Beads with stronger adsorption capability appeared to result in some destruction in the crystalline arrays and vesicle structures (Fig. 3d).

Though small in size, 2D crystalline arrays of GusB were obtained from the Bio-Beads methods with DMPC as an additional lipid at the lipid to protein ratio of 1.1 after 2 h- incubation at 28.9 °C (Fig. 4). Figure 4a shows the electron micrographs of the negatively stained 2D crystals of GusB and Fig. 4b is its Fourier-transformed image. Reversed Fourier-filtered image is shown as Fig. 4c. The crystals form a hexagonal lattice with the layer group *P*6, and unit cell parameters of $a = b = 13.75$ nm, $\gamma = 120°$. This is the first observation of GusB in 2D crystalline form at such quality.

Discussion

Although single particle reconstruction method has been applied for many monodispersed proteins (complexes) having rather large molecular masses (Lau and Rubinstein 2012), this is another approach to determine protein structures by electron microscopy. The capability to determine protein structures by electron crystallography is limited by the fact that the techniques for producing 2D crystals have not advanced as rapidly as the methods for electron microscopy and computation for 3D reconstruction. Despite the ever increasing number of thin crystals of membrane proteins, the major limitation of the electron microscopy approach has been the preparation of specimens with the required structural order and size for diffraction and imaging. Thus, the most challenging obstacle in obtaining crystalline images and diffraction data at high resolution is related to the quality and size of 2D crystals. We have sought a promising approach for preparing 2D crystals of GusB protein, and have come across a simple method that Rigaud et al. (1997, 2000) reported almost a decade ago. If we could succeed in optimizing the parameters concerned, it appeared to be a promising approach. As Rigaud et al. (1997) reported, there is a linear relationship between the rate of the detergent removal and the number of beads present in solution, regardless of the

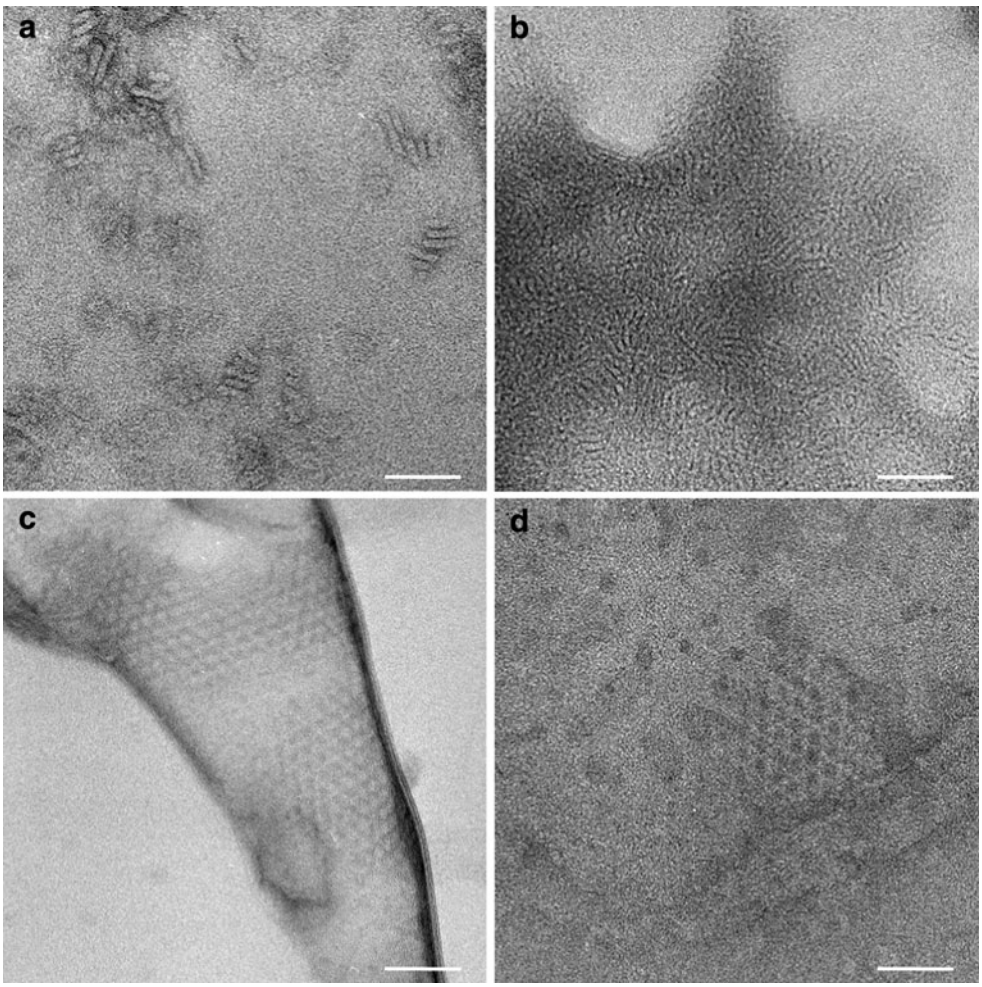

Fig. 3 Electron micrographs at each stage during the incubation with Bio-Beads. **a** Freshly prepared GusB protein in 0.1 % DDM, stacked layered structures are seen. **b** At the stage before the addition of Bio-Beads, all components of the membrane protein GusB, detergent (DDM), and lipid (DMPC) are seen gathered 2-dimensionally. **c** After 2 times of 30-min incubation with Bio-Beads, vesicles containing some regions of crystallinity of the transporter were observed. **d** Prolonged incubation led to result in some destruction in the crystalline arrays and vesicle structures. *Scale bar* = 50 nm

initial detergent concentration. This reveals that a limiting factor in the rate of detergent removal is the availability of the adsorptive surface of Bio-Beads SM2. This adsorptive property can be exploited to control the rate of detergent removal. In addition to the large number of parameters that artificially affect the formation of 2D crystals such as temperature, buffer composition and pH, and lipid-to-protein ratios, detergent removal is a key step because it controls the micelle-to-bilayer phase transition and the protein incorporation into the lipid bilayer and its 2D array formation (crystallization).

In the 2D crystallization of GusB, the effects of pH and buffer species on the stability of GusB led us to some similar conditions where the small 2D crystalline arrays were obtained at a lipid (DMPC) to protein ratio of 1.1 at 28.9 °C. For the incubation temperature, 2D crystallization experiments need often to be performed at as low temperature as possible to avoid possible protein denaturation, and at the same time the fluidity of the lipids must be considered. We found that acetate buffer and citrate buffer appeared to help the stability of GusB, whereas MES and HEPES buffer made GusB unstable, and that GusB was stable at pH 7.2 and lower, but not at pH 7.4 and higher even in the presence of DMPC. As lipids have normally two hydrocarbon tails, they form a stable hydrophobic scaffold (bilayer) that is more favorable configuration for the incorporation of integral membrane proteins than detergent micelles. This effect in the membrane-spanning region seems to contribute to the stabilization of the extramembraneous region through the defined subunit–subunit interactions.

However, when the protein stability was checked after prolonged incubation at 25 °C, we noticed that DMPC made GusB unstable after 1–5 days, which is the time scale

usually needed for 2D crystallization. This indicates that the incubation with DMPC for 1–2 h sometimes promotes 2D crystallization of GusB, but that further incubation with DMPC for several days does harm to GusB. Though acidic conditions at pH 6.5 and lower do not destabilize GusB, the pH regions between 6.5 and 6.9, and at 7.4 and higher adversely affect the stability of GusB. GusB produced small 2D crystals with DMPC, but longer incubation with DMPC might destabilize GusB. Thus, other lipids that may help stabilize GusB need to be investigated.

It has been shown that many bacteria change the fatty acid composition of their cell membrane to maintain the optimum fluidity in response to environmental temperature; the relative amount of long, straight, and saturated fatty acid increases with temperature elevation. Approximately 65–85 % of native *E. coli* lipids consist of PE, and its ability to maintain activities of incorporated membrane proteins has been reported (Chen and Wilson 1984; Seto-Young et al. 1985). We observed the effect of *E. coli* total lipids extracts on the stability of GusB. *E. coli* total lipids extracts greatly helped to stabilize GusB. Furthermore, the incubation for 30 days with *E. coli* total lipids extracts in citrate buffer (pH 5.5) preserved GusB at the level of 80 % of initial amount, whereas the incubation without the *E. coli* total lipids extracts reduced the amount of intact protein to half of the initial amount within 9 days. Nevertheless, any 2D crystals of GusB were not obtained with *E coli* total lipids extracts by the Bio-Beads method. GusB is originated from *E. coli* membrane; thus, GusB appears to prefer the environment with *E. coli* total lipids extracts. Approximately 65–85 % of *E. coli* membrane is composed of PE. Although PE and PC have similar molecular structure, they form an extremely different molecular assembly in solution. This is due to the difference in rate that the volume occupies within the molecule of the polar head group of a phospholipid and the nonpolar group such as fatty acid. The balance of the volume occupied by polar and nonpolar domains is good in PC and is called cylinder type lipid. Therefore, PC forms a stable bilayer membrane structure in solution. On the other hand, the proportion of nonpolar portion is large compare to the polar portion in PE; thus, PE is called a cone-shaped lipid. Its characteristic destabilizes the stable bilayer structure. These features are consistent with the fact that *E. coli* total lipids extracts fail to yield 2D crystalline arrays, although they could stabilize GusB.

As seen in Fig. 4, each stain-protruding periodic unit showed approximately 11.8 ± 0.3 nm in diameter in the inverse Fourier-filtered image and is in good agreement with the projection image assumed to have been formed by an oligomer where the pentameric GusB (5 × 49.7 kDa) resides. Structural information in further detail from 2D or 3D crystals of GusB is requisite to understand the substrate specificity as well as its functional mechanism and to discover the translocation pathway in the protein. As the protein–detergent complex is the species that crystallize, understanding its characteristics and behavior in solution has become especially important. Detergent-protein and detergent-lipid interactions may play a critical role in the initial stage. The amount of detergent bound to the protein surface varies depending on detergent characteristics (type, concentration, etc.), solved environment (pH, ionic

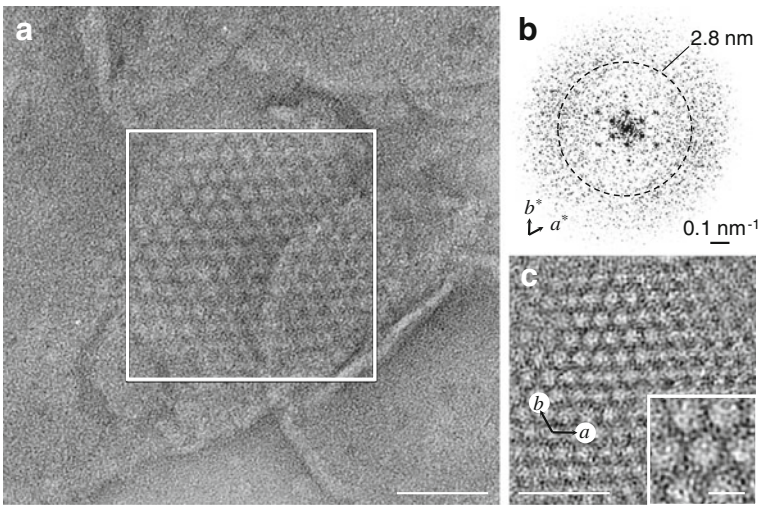

Fig. 4 **a** Electron micrographic image of 2D crystalline array of GusB. *Scale bar* = 50 nm. **b** Computed diffraction pattern of the 2D crystalline array of GusB indicated with a *box* in (**a**). The *a**- and *b**-axis of the hexagonal lattice are indicated. The *dotted circle line* corresponds to a spacing of 2.8 nm. Diffraction bar is 0.1 nm^{-1}. **c** Fourier-filtered image of 2D crystalline array showing the diffraction pattern in (**b**). All diffraction spots were masked off with Gaussian-shaped circular masks and were inverse Fourier transformed. $a = b = 13.75$ nm, and $\gamma = 120°$. *Scale bar* = 50 and 10 nm for the enlarged *inset*

strength, etc.), and of course the protein. In solution, the protein bound detergent appears to be distributed as a uniform band or torus mass about the protein surface, presumably covering the hydrophobic, transmembrane region. Choosing a detergent for solubilization and manipulation of a membrane protein thus depends on its ability to maintain the native structure and function of the protein, its effectiveness in delipidating the protein, and its capability for maintaining the protein in a stable state preserving solubility. A typical membrane protein appears to possess bound detergents between 40 and 60 % of its weight in detergent. In order for a protein molecule bound to a torus-shaped detergent to be incorporated into a liposome made from a desired lipid, the interaction between the lipid and the detergent has to be carefully optimized. In this article, we examined the basic strategies with Bio-Beads method for setting up 2D crystallization experiments, and succeeded in producing 2D crystalline array formation with GusB protein from detergent-solubilized preparations in the presence of DMPC.

Acknowledgments The author would like to express thanks to Prof. R. M. Glaeser for stimulating discussion, and Drs. F. M. Hendrickson and K. S. Kim for discussions and critical reading. The part of the research was financially supported by the Overseas Research Fellowship from Japan Science and Technology Corporation.

References

Chen CC, Wilson TH (1984) The phospholipid requirement for activity of the lactose carrier of *Escherichia coli*. J Biol Chem 259:10150–10158

Fujiyoshi Y (2011) Electron crystallography for structural and functional studies of membrane proteins. J Electron Microsc 60:S149–S159

Henderson PJF (1993) The 12-transmembrane helix transporters. Curr Opin Cell Biol 5:708–721

Hirokawa T, Boon-Chieng S, Mitaku S (1998) SOSUI: classification and secondary structure prediction system for membrane proteins. Bioinformatics 14:378–379

Ishii N (2010) Investigation on stability of transporter protein, glucuronide transporter from *Escherichia coli*. J Membr Biol 235:63–72

Ishii N (2011) Erratum to: investigation on stability of transporter protein, glucuronide transporter from *Escherichia coli*. J Membr Biol 240:171

Lau WCY, Rubinstein JL (2012) Subnanometre-resolution structure of the intact *Thermus thermophilus* H^+-driven ATP synthase. Nature 481:214–219

Liang WJ, Wilson KJ, Xie H, Knol J, Suzuki S, Rutherford NG, Henderson PJF, Jefferson RA (2005) The *gusBC* genes of *Escherichia coli* encode a glucuronide transport system. J Bacteriol 187:2377–2385

Poolman B, Modderman R, Reizer J (1992) Lactose transport system of *Streptococcus thermophilus.* The role of histidine residues. J Biol Chem 267:9150–9157

Pourcher T, Leclercq S, Brandolin GK, Leblanc G (1995) Melibiose permease of *Escherichia coli:* large scale purification and evidence that H^+, Na^+, and Li^+ sugar symport is catalyzed by a single polypeptide. Biochemistry 34:4412–4420

Rigaud JL, Mosser G, Lacapere JJ, Olofsson A, Levy D, Ranck JL (1997) Bio-Beads: an efficient strategy for two-dimensional crystallization of membrane proteins. J Struct Biol 118:226–235

Rigaud JL, Chami M, Lambert O, Levy D, Ranck JL (2000) Use of detergents in two-dimensional crystallization of membrane proteins. Biochim Biophys Acta 1508:112–128

Saier MH Jr, Beatty JT, Goffeau A, Harley KT, Heijne WHM, Huang SC, Jack DL, Jähn PS, Lew K, Liu J, Pao SS, Paulsen IT, Tseng TT, Virk PS (1999) The major facilitator superfamily. J Mol Microbiol Biotechnol 1:257–279

Sato MH, Kasahara M, Ishii N, Homareda H, Matsui H, Yoshida M (1994) Purified vacuolar inorganic pyrophosphatase consisting of a 75-kDa polypeptide can pump H^+ into reconstituted proteoliposomes. J Biol Chem 269:6725–6728

Seto-Young D, Chen CC, Wilson TH (1985) Effect of different phospholipids on the reconstitution of two functions of lactose carrier of *Escherichia coli*. J Membr Biol 84:256–267

Vinothkumar KR, Henderson R (2010) Structures of membrane proteins. Q Rev Biophys 43:65–158

Yazyu H, Shiota-Niiya T, Shimamoto T, Kanazawa H, Futai M, Tsuchiya T (1984) Nucleotide sequence of the melB gene and characteristics of deduced amino acid sequence of the melibiose carrier in *Escherichia coli*. J Biol Chem 259:4320–4326

Yousef MS, Guan L (2009) A 3D structure model of the melibiose permease of *Escherichia coli* represents a distinctive fold for Na^+ symporters. Proc Nat Acad Sci USA 106:15291–15296

Zamek-Gliszczynski MJ, Hoffmaster KA, Nezasa K, Tallman MN, Brouwer KLR (2006) Integration of hepatic drug transporters and phase II metabolizing enzymes: mechanisms of hepatic excretion of sulfate, glucuronide, and glutathione metabolites. Eur J Pharm Sci 27:447–486